Alterations in Cellular Metabolome after Pharmacological Inhibition of Notch in Glioblastoma Cells

Ulf D Kahlert[1,2,*], Menglin Cheng[3], Katharina Koch[2], Luigi Marchionni[4,7], Xing Fan[5], Eric H Raabe[6,7], Jarek Maciaczyk[2], Kristine Glunde[3,7] and Charles G Eberhart[1,*]

[1] Department of Pathology, Division of Neuropathology, Smith Research Building, 400 North Broadway, Johns Hopkins Hospital, Baltimore, MD 21287, USA;

[2] Department of Neurosurgery, University Medical Center, Forschungsgebaeude Pathologie, Moorenstr. 5, 40225 Düsseldorf, Germany;

[3] Division of Cancer Imaging Research, Russell H. Morgan Department of Radiology and Radiological Science, Traylor Building Room 212, 720 Rutland Avenue, Johns Hopkins Hospital, Baltimore, MD 21205, USA;

[4] Department of Oncology, Cancer Research Building 2, 1550 Orleans Street, Johns Hopkins Hospital, Baltimore MD, 21231, USA;

[5] Departments of Neurosurgery and Cell and Developmental Biology, 109 Zina Pitcher Place, 5018 BSRB, University of Michigan, Ann Arbor, MI 48109-2200, USA;

[6] Department of Pediatric Oncology, Smith Research Building, 400 North Broadway, Johns Hopkins Hospital, Baltimore, MD 21287, USA;

[7] Sidney Kimmel Comprehensive Cancer Center, Johns Hopkins University School of Medicine, Baltimore, MD 21231, USA

*** corresponding authors:**

Charles G Eberhart, ceberha@jhmi.edu and Ulf D Kahlert, ulf.kahlert@gmx.de

720 Rutland Ave – Ross Bldg. 558, Baltimore, MD 21205, Phone: 410-502-5185, Fax: 410-614-3457

Total word count without references: 4103

Novelty:

We provide initial evidence that Notch inhibition using a gamma secretase inhibitor (GSI) changes multiple aspects of the cellular metabolome in brain tumors. These changes in glioblastoma neurospheres included reduced intracellular glutamate, which was not seen when treating with other chemotherapeutic agents, or in human neural stem cells after Notch inhibition. Alterations in glutamate metabolism may represent a mechanism by which Notch modulates brain tumor growth and have diagnostic or therapeutic utility.

Abstract:

Notch signaling can promote tumorigenesis in the nervous system and plays important roles in stem-like cancer cells. However, little is known about how Notch inhibition might alter tumor metabolism, particularly in lesions arising in the brain. The gamma-secretase inhibitor MRK003 was used to treat glioblastoma neurospheres, and they were subdivided into sensitive and insensitive groups in terms of canonical Notch target response. Global metabolomes were then examined using proton magnetic resonance spectroscopy, and changes in intracellular concentration of various metabolites identified which correlate with Notch inhibition. Reductions in glutamate were verified by oxidation-based colorimetric assays. Interestingly, the alkylating chemotherapeutic agent temozolomide, the mTOR-inhibitor MLN0128, and the WNT inhibitor LGK974 did not reduce glutamate levels, suggesting that changes to this metabolite might reflect specific downstream effects of Notch blockade in gliomas rather than general sequelae of tumor growth inhibition. Global and targeted expression analyses revealed that multiple genes important in glutamate homeostasis, including glutaminase, are dysregulated after Notch inhibition. Treatment with an allosteric inhibitor of glutaminase, compound 968, could slow glioblastoma growth, and Notch inhibition may act at least in part by regulating glutaminase and glutamate.

Introduction:

Glioblastoma (GBM) are one of the most lethal cancers [1], and a subpopulation of cells generally known as glioma stem cells (GSCs) are thought to be major drivers of tumor progression and therapeutic resistance [2]. Molecular regulators of GSCs therefore represent potential therapeutic or diagnostic targets. Suppression of developmental signaling cascades important in non-neoplastic stem cells has emerged as a promising strategy to target stem-like cells in cancers [3], and one such pathway is Notch.

Notch regulates numerous processes during embryonic and adult development, [4] including neural stem cell biology, [5] and its oncogenic role has been demonstrated in many tumors outside the brain [6] as well as in GBM [7]. The importance of understanding the effect of key oncogenes on the cellular metabolome in cancer is becoming increasingly appreciated [8]. Recent studies suggest that Notch can regulate cellular metabolism in normal tissues [9–11], and in some tumors outside the brain such as leukemia [12] or breast cancer [13]. However, little is known about the effects of Notch on the metabolism of brain tumors including GBM.

We therefore examined the effects of Notch inhibition on the global metabolome in GBM neurospheres. Prior studies have shown that pharmacological inhibition of the enzyme gamma-secretase, responsible for terminal activating cleavage of the Notch receptor, effectively targets the stem-like cell population in GBM [14]. The gamma-secretase inhibitor MRK003 was therefore used to treat GBM neurospheres sensitive to Notch blockade in terms of pathway suppression, as well as insensitive control lines. Inhibition of Notch activity caused a range of metabolic changes in the GBM cells as measured by high-resolution proton nuclear magnetic resonance spectroscopy (^{1}H-NMR), including phosphocholine as well as metabolites associated to glycolysis and glutaminolysis. Given the previously reported important role of glutamate in gliomagenesis [27] we decided to focus our studies on this metabolite and found decreased levels of intracellular glutamate in glioma cells after Notch blockade. This was not observed after treatment with pharmacological compounds

suppressing WNT or mTOR signaling, or by the alkylating agent temozolomide, suggesting that these changes are not the generic result of tumor growth inhibition or modulation of signaling cascades important in GSCs. Moreover, treating MRK003 sensitive cells with the glutaminase inhibitor compound 968 reduced their overall growth, but not that of MRK003 insensitive cells.

Material and Methods:

Cell lines and cell culture

The GBM1 and 040922 lines were derived as previously described, and generously provided by Dr. Vescovi [14]. GBM10 [15] and GBM14 [16] were established in our laboratory from intraoperative tumor specimens obtained from the Department of Neurosurgery, Johns Hopkins Hospital. U87 and LN229 were purchased from American Tissue Culture Collection (www.atcc.com). All cells where cultured as neurospheres (NS) in serum-free and glutamine rich conditions as described before [15], and passaged at least twice per week, except for LN229, which was propagated in Dulbecco´s Modified Eagle Medium (DMEM, Life Technologies, NY, USA) supplemented with 10% fetal calf serum (Life Technologies).

Human fetal neural stem cells (fNCS) were obtained from first trimester human fetal autopsy specimens as described [17] in concordance with German law and Ethics Board evaluation (Division of Stereotactic Neurosurgery, University Medical Center Freiburg, Germany) and cultured as neurospheres. This study was also approved by the Johns Hopkins Institutional Review Board. Cell line identity was confirmed for all cultures by analysis of nine short tandem repeats (STR) plus a gender determining marker, Amelogenin using the StemElite kit (Promega, Madison, WI, USA) in the John Hopkins Core Facility for DNA fragment analyses (Supporting Data File S1).

Suppression of the NOTCH pathway

12 hours prior to the start of the experiments, cultures were dissociated to single cell suspension and plated at a concentration of $1.5x10^6$ cells per 1ml of media to ensure exponential growth status. The next day, media was replaced with media containing the gamma-secretase inhibitor MRK003 (Merck Research Laboratories, NJ, USA) or Dimethyl Sulfoxide (DMSO, #D9170, Sigma-Aldrich, MO, USA) as vehicle control. Based on our previous experience with MRK003 [14], we applied MRK003 in a final concentration of 1µM for 48 hours to achieve significant pathway inhibition as confirmed by reduction of canonical

target genes (*HES1* and *HEY1*) expression but only low to moderate cell death. With this treatment regime, we aimed to minimize secondary effects on the metabolome introduced through cell degradation.

Extraction and quantification of metabolites from *in vitro* cultures using high resolution proton nuclear magnetic resonance spectroscopy (^{1}H-NMR)

Cells were harvested, washed twice in 1xPBS (Life Technologies) and quantified using Trypan blue (#T8154, Sigma-Aldrich) exclusion assay (3 independent counts). A minimum of $7*10^6$cells per sample were used for each extraction and total cell numbers where used to normalized between MRK003 and DMSO counterparts. The methanol-chloroform-water (1/1/1, v/v/v, all Sigma-Aldrich) dual phase cell extraction protocol was applied to obtain water and lipid-soluble metabolites as previously described [18]. The lyophilized water-soluble extracts were resolved in 495µl deuterium oxide (D_2O, #151882, Sigma-Aldrich) supplemented with 5µl D_2O containing 0.05% 3-(trimethylsilyl)propionic-2,2,3,3,-$d_4$acid (TSP, #450510, Sigma-Aldrich) as internal concentration standard. The extracts were analyzed in the Department of Radiology, Johns Hopkins Hospital on a Bruker Avance 500 spectrometer operating at 11.7 T using a 5-mm HX inverse probe run at 25°C as previously described [18]. The fully relaxed ^{1}H-NMR data were post-processed and metabolites quantified through peak integration using Mestrenova v10.0 (Mestrelab Research, CA, USA). For each sample, Notch activation status was assessed by quantification of canonical target gene expression.

ELISA based quantification of glutamate

Colorimetric quantification of glutamate was performed through glutamate dehydrogenase-mediated oxidation using EnzyChrom™ Glutamate Assay Kit (EGLT-100, BioAssay Systems, CA, USA) according to the manufacturers' protocol. Each step of sample preparation was performed on ice if not mentioned otherwise. In brief, cells were harvested, washed 2 times in 1xPBS (Life Technologies) and lysed in 1xPBS containing 1xproteinase

inhibitor (#P2714-1BLT, Sigma-Aldrich). Cell membranes were broken through a 3-times performed freeze-thaw cycle using a dry-ice/ethanol bath and a water bath warmed to 37 °C. Total protein concentration determined by Protein Assay Dye Reagent (#500-0006, Bio-Rad, CA, USA) was used to normalize the individual samples of each group. Absorptions reflecting concentrations of total protein (595nm) as well as glutamate (565nm) were measured on an Epoch plate reader (BioTek Instruments, VT, USA).

Whole genome expression profiling

Whole human genome gene expression was measured as described before [19] using 44k microarray technology (Agilent Technologies, CA, USA) based assessment performed at the Johns Hopkins Oncology Microarray Core, with labeling, hybridization and detection performed according to the manufacturer's instructions (Agilent Technologies). All analyses were performed using software packages available from the R/Bioconductor platform for statistical computing. Briefly, we used a generalized linear model approach for differential gene expression detection, and performed gene set enrichment analysis using Analysis of Functional Annotation, as previously described [20]. Similarly, all processes for gene annotation, raw expression data and MIAME (Minimal Information about a Microarray Experiment) have been described by our lab before [19]. We considered genes with a false discovery rate of <5% as differentially regulated. The data can be accessed through the NCBI GEO data portal under http://www.ncbi.nlm.nih.gov/geo/query/acc.cgi?acc=GSE71769.

Targeted gene expression analyses and Western blot

The relative abundance of gene transcripts was determined using SYBR-green based ddCt-method on an IQ^{TM}5-system (Bio-Rad) normalized to beta-actin housekeeping gene expression. The sequences for the primers used in this study are listed in Supporting Data File S2. For Western blotting we used anti-glutaminase antibody #12855-1-AP (Proteintech, IL, USA, 1:1000) and anti-beta-Actin antibody #sc-47778 (Santa Cruz Biotechnology, TX, USA, 1:1000).

Analyses of cellular growth and apoptosis

For all assays, cells were dissociated to single cell suspension and viable cells quantified using the MUSE Count & Viability Assay Kit (#MCH100102, Merck KGaA) on a Muse Cell Analyzer (#0500-3115, Merck KGaA). For growth studies, 5000, 10 000 or 20 000 cells (dependent on cell line and assay) were plated in a 96 well in 100µl triplicates. Biologically active cell mass was then measured using the TiterBlue assay (#G8081, Promega, Madison, WI, USA) according to the manufacturer's description on an Infinite M1000Pro plate reader (Tecan, Morrisville, NC, USA). Cell Titer Blue reagent (20µl/well) was added directly to the cells, incubated for two hours at 37 °C followed by fluorescence intensity measurement at 560ex/590em nm.

Apoptotic cells were quantified using the AnnexinV & Dead Cell Kit (#MCH100105, Merck KGaA, Darmstadt, Germany) on the Muse Cell Analyzer according to manufactures protocol. A minimum of 2000 gated events were acquired.

Additional pharmacological treatment

All pharmacological treatment experiments required the dissociation to single cells before the start of the experiment ($1.5x10^5$ NS cells per 1ml of media, $3.5x10^5$ cells LN229 per cm^2 culture area). We treated the cells in the indicated concentrations with the alkalyting agent Temozolomid [1] (TMZ, #T2577, Sigma-Aldrich), dual TORC1/2 inhibitor INK-128/Milenum0128 [21] (MLN, #S2811, www.selleckchem.com), porcupine inhibitor LGK974 to interrupt WNT ligand/receptor interaction [22] (Xcess Biosciences, San Diego, CA, USA, #M60106-2S) and glutaminase inhibitor compound 968 [23] (Millipore, #352010). The indicated drug concentrations diluted in growth media were compared to the individual vehicle control (DMSO).

Determination of WNT/beta-catenin pathway activity

WNT/beta-catenin pathway inhibition through LGK974 was confirmed through

bioluminescence-based quantification of occupied putative beta-catenin T cell factor/lymphoid enhancer factor (TCF/LEF)-binding sites using the stable integration of 7TFP *firefly* luciferase reporter as described before [24]. Infectious lentiviral particles were generated using the 3rd generation lentiviral packaging system and stable integration was selected through puromycin (Sigma- Aldrich) resistance at a concentration of 2ug/ml.

For each measurement, cells were harvested, washed in 1xPBS and lysed according to the manufacturer's descriptions using the Dual-light combined Luciferase & beta-Galactosidase Reporter Gene Assay System (#T1003, Life Technologies). Luminescence was read at an emission wavelength of 490nm on the Infinite M1000Pro plate reader (Tecan) and normalized to beta-galactosidase activity. A robust IC_{50} was achieved at 5μM LGK974 at 48 hours as defined by previous experiments [25].

Figure generation

Sigma Blot 8.0 (Systat Software, San Jose, CA), Prism v5 (GraphPad Software La Jolla, CA) and Illustrator C4 (Adobe System, San Jose, CA) were used to generate the figures.

Statistical evaluation

Statistical analyses were performed using a two-tailed Students t-Test and presented as mean values plus standard deviation if not indicated otherwise. P-values ≤0.05 were considered statistically significant.

Results:

Altered metabolic profiles in glioma neurospheres after Notch suppression

It has been shown that while some GBM are sensitive to GSIs, others are resistant to Notch blockade [26]. mRNA levels of the canonical Notch pathway targets *HES1* and *HEY1* were measured to confirm sensitivity or resistance in five glioma lines. Four of these were originally derived as neurospheres, while U87 was continuously passaged as neurospheres in serum free media for these studies and designated as U87NS. Significant suppression of mRNA levels for several direct transcriptional targets of Notch were achieved in the GBM1, GBM10 and GBM14 lines, but not in U87NS or 040922 cells (Figure 1A, $p \leq 0.05$). Based on this, we classified GBM1, GBM10, and GBM14 as MRK003 sensitive, with U87NS and 040922 designated MRK003 insensitive.

High resolution proton nuclear magnetic resonance spectroscopy (^{1}H-NMR) was used to compare metabolic changes in MRK003 sensitive and insensitive lines. While this technique allows for precise identification and quantification, it requires extremely large numbers of cells, thus the initial survey was performed on only the two fastest growing lines in each group, GBM1 and U87NS. The levels of GSI used for these studies resulted in a modest induction of apoptosis for GBM1 and had no effect AnnexinV in the other tested cell lines. (Figure 1B, $p \leq 0.05$).

We identified a broad range of metabolites with characteristic peak formations of singulet (S), duplet (D) or multiplet (M), including valine/ isoleucine (Val/Iso) at 0.9-1.0ppm (M), threonine (Thr) at 1.30ppm (D), lactate (Lac) at 1.33ppm (D), alanine (Ala) at 1.47ppm (D), N-Acetylaspartylglutamat (NAAG) at 2.05ppm (S), glutamate (Glu) at 2.33ppm (M), glutamine (Gln) at 2.41ppm (M), glutathione (GSH) at 2.50ppm (M), total creatine (tCre) at 3.03ppm (D), free choline (fCho) at 3.18ppm (S), phosphocholine (PC) at 3.22ppm (S), glycerophosphocholine (GPC) at 3.24ppm (S), glycine (Gly) at 3.55ppm (S) and *myo*-inositol (myo) at 4.05ppm (M). Representative findings are shown in Figure 2A, and the summary of

three independent experiments in each of the two lines in Figure 2B. Interestingly, while a number of metabolite levels decreased after Notch blockade in the sensitive GBM1 cells, no corresponding decreases were seen in MRK003 insensitive U87NS except for myo-inositol (Figure 2B). Significant decreases were noted in glutamate, glutamine, free choline, phosphocholine after Notch pathway inhibition. Myo-inositol levels also decreased in the GBM1 and significantly reduced in U87NS cells after GSI treatment. Due to technical issues in one GBM1 repetition only two of the three independent samples could be quantified for this metabolite, and therefore no statistical comparison of myo-inositol was performed in these cells. Interestingly, while no other significant decreases in metabolite levels were seen in U87NS cells, threonine and lactate levels were significantly increased.

Reduction of glutamate after Notch inhibition

We focused on changes to glutamate, and Figure 3A shows a more detailed view of a representative spectra of this region, with a 36% mean reduction ($p \leq 0.05$) in GBM1 cells as compared to a non-significant 7% increase in U87NS cells after Notch inhibition. To verify this observation and extend it to additional lines, we used an ELISA-based method based on oxidation of glutamate, which was more easily performed on small samples. This confirmed that Notch pathway suppression reduced intracellular glutamate levels by 50% and 26% in the GSI sensitive lines GBM1 and GBM10 ($p \leq 0.05$).No glutamate reduction was noted in the insensitive U87NS and 040922 neurospheres (Figure 3B). In addition, while MRK003 inhibited Notch in human fetal cortical neurospheres, it did not reduce levels of intracellular glutamate (Figure 3C), suggesting that the observed Notch-glutamate interplay is differentially regulated in non-neoplastic neural stem cells.

Treatment with other chemotherapeutics did not reduce glutamate

To determine if the observed glutamate reduction might be a general consequence of treatment, we examined the effect of other pharmacological agents on glutamate levels. The standard alkylating agent temozolomide (TMZ) and the mTOR inhibitor INK-128/MLN0128 (MLN) were tested on the MRK003 sensitive cell lines GBM1 and GBM10. Both TMZ and MLN caused a profound decrease in cellular growth (Figure 4A), and after 48 hours apoptosis in GBM1 was induced to a degree similar to that seen with MRK003, but no corresponding glutamate reduction was detected in these samples (Figure 4B). Thus chemotherapeutic growth inhibition and increased apoptosis is not always associated with glutamate alterations in glioma neurospheres.

We also examined if other pathways important in non-neoplastic and glioma stem cells might regulate glutamate. A number of groups have shown that WNT signaling blockade depletes stem-like glioma cells [28]. We have recently shown that the porcupine inhibitor LGK974, which targets WNT signaling by modulating ligand processing, can also inhibit the pathway and reduce survival in glioma neurospheres[25]. For these LGK974 studies, LN229 cells were used instead of GBM10, as LN229 is characterized by higher WNT activity similar to that seen in the upper range of snap frozen GBM specimens [25]. Inhibition of the pathway after LGK974 administration was confirmed by reduction in luciferase WNT reporter signals, with no corresponding effects on glutamate levels (Figure 4C).

Notch blockade alters expression of multiple regulators of glutamate homeostasis

In order to determine the mechanism by which Notch was altering glutamate levels, we examined global transcriptomes from MRK003 sensitive GBM1, GBM10 and GBM14 cells after 2μM MRK003 treatment. This identified a number of dysregulated genes important for glutamate homeostasis, which are listed in Figure 5A. To confirm this, we performed targeted gene expression analysis via RT PCR for a panel of core regulators of cellular glutamate metabolism in our cell lines. This includes NAAG-cleaving glutamate

carboxypeptidase II (*GCPII*), a member of the soluble carrier (SLC) membrane transporter family responsible for intracellular glutamate uptake (*SLC1A3*) as well as the glutamine to glutamate hydrolyzing glutaminase (*GLS1*) (Figure 5B).

Drug treatment significantly reduced the expression of *GCPII* in the MRK003 sensitive GBM1 (40%) and GBM14 (20%) cultures but not in MRK003 insensitive U87NS or 040922 cells. No *GCPII* transcription was detected in GBM10. *SCL1A3*, which helps import glutamate into the cell, was significantly reduced in most MRK003 sensitive lines after Notch blockade, but not in MRK003 insensitive ones. Interestingly, while MRK003 sensitive cells expressed higher baseline levels of glutaminase as compared to insensitive cells (Figure 5C), they were the only ones to show a decrease in *GLS1* mRNA after Notch blockade (Figure 5B).

Treatment with inhibitor of glutaminase reduced cell growth

If reductions in glutamate represent a major mechanism through which Notch blockade slows glioma growth, one would predict that direct inhibition of this metabolic pathway would have a similar effect. We therefore treated our neurosphere cultures with the glutaminase inhibitor compound 968 [23] and observed significant growth inhibition in MRK003 sensitive lines, while no effect was seen on growth of MRK003 insensitive cultures (Figure 6A). A similar pattern of response in MRK003 sensitive cells was seen when less selective glutaminase inhibitors such as Acivicin or 6-Diazo-5-oxo-L-norleucine (DON) were used (data not shown). No additive effect was seen after combination treatment with both MRK003 and compound 968 (Figure 1B).

Discussion:

Despite the importance of Notch in normal development [29] and oncogenesis [6,7] little is known about how this signaling cascade can regulate cell metabolism. Our data indicate that pharmacological Notch blockade alters intracellular levels of a range of metabolites in glioma cells. In general, we saw decreased metabolite levels, while treatment of neurospheres insensitive to Notch inhibitor MRK003 show no reductions in these metabolites.

Notch blockade significantly reduced the onco-metabolite phosphocholine (PC). PC has been found to be particular high in fast dividing glioma cells [30] and elevated in malignant high grade brain tumors as compared to low grades [31,32]. Moreover, PC has been shown to be downstream of mTOR in GBMs [33,34], and our data now adds a link to Notch. Additionally, our NMR studies showed the MRK003 treatment led to reduction of glycine (gly) in both MRK003 insensitive and sensitive GBMs reaching statistical significance in the latter. Of note, gly has recently been shown to be involved in the regulation of survival of hypoxic glioma cells[35], a population of cells particular enriched with stem-like characteristics [36], and is known to be positively associated to rapid cancer cell proliferation [37]. Furthermore, we found lactate, an indicator of active glycolysis, to be increased after treatment with the Notch inhibitor in both glioma subgroups. This is concordant with very recent discoveries that Notch stimulates cellular anaerobic glucose metabolism in breast cancer [13] and during macrophage activation [38].

Besides these alterations, we found a significantly different response in the two glioma groups after drug treatment in terms of intracellular glutamine (gln) and glutamate (glu), as we detect significant lower levels of these two metabolites in MRK003 sensitive GBM1 but not in MRK003 insensitive U87NS after treatment. We focused in particular on changes to glutamate, given the many prior studies implicating it in the biology of brain tumors [27] and confirmed its reduction after Notch blockade with oxidation based quantifications. These changes may be linked to increased differentiation of the tumor.

It has previously been shown that differentiated glioma cells possess lower levels of glutamate as compared to stem-like GBM cells [39] and high levels of intracellular glutamate in glioma neurospheres are associated with increased clonogenicity as well as with increased expression of glioma stem cell (GSC) marker CD133 [40]. Moreover, Angulo-Rojo and colleagues found that Notch induces glutamate consumption during terminal differentiation of astrocytes [41]. Glutamate has also been shown to serve as growth stimulus for murine GSCs and that the neocortex, a brain region rich in glutamate, generates a metabolic niche advantageous for the growth of brain tumors [42].

Our findings are consistent with prior studies implicating Notch in glutamate regulation. For example, glutamate levels are particular high in glioma cells clustering with the PDGFRA+ signature of proneural GBMs [43] – the subset of gliomas with high Notch activation [63]. This glutamate accumulation is thought to possibly be due to overactive glutamate uptake mediated through the members of the soluble carrier (SLC) membrane transporters family. [43] However, further studies are needed to determine whether the lowered glu level in our cells is a consequence of altered consumption or production.

Regardless of the mechanism by which glu is regulated by Notch, it appears to be a promising therapeutic target. We found that Notch blockade suppressed transcript levels of cardinal glutaminolysis regulator glutaminase (GLS). GLS is known to promote cancer cell proliferation [44,45] and its suppression can impair tumor growth. Previously, genetic GLS suppression slowed GBM growth, and pharmacological suppression with BPTES preferentially acted on glioma cells with mutant isocitrate dehydrogenase 1 (*IDH1*) [46]. We treated our cells with the recently discovered GLS inhibitor compound 968 [23], which acts through a different principle of allosteric inhibition as compared to BPTES [47]. This suppressed growth of MRK003 sensitive cells which were not *IDH1* mutant, but failed to slow growth of MRK003 insensitive cells. Therefore, our data indicate that GLS suppression in some GBMs can have anti-growth benefits independent of *IDH1* status, and suggest that the therapeutic benefit of MRK003 [14] might be, at least in part, mediated by interference with

glutamate/glutamine metabolism. This is supported by the observation that the addition of compound 968 to MRK003 did not result in an increased antigrowth effect, suggesting that they may be acting via a common mechanism.

Importantly, the commonly used chemotherapeutic agent TMZ, the inhibitor of mTOR signaling MLN, and the WNT inhibitor LGK974 could reduce cellular growth and induce apoptosis, but did not reduce glutamate in the same fashion as Notch blockade, suggesting that this change was not a general effect of all agents targeting brain tumors. Interestingly, glioma cells resistant to mTOR inhibition have recently been shown to induce glutamine metabolism as compensatory pro-survival strategy resulting in elevated intracellular glutamate [48], although we do not see signs of this in our lines after 48 hours treatment with MLN.

Taken together, our data suggest that Notch blockade can have widespread effects on brain tumor cellular metabolism, including glycolysis, glycine- and choline- metabolism as well as glutaminolysis, which extend beyond simple manifestations of growth inhibition. It should be noted that Notch inhibition was achieved pharmacologically, and the possibility of off-target effects of MRK003 on glutamate or other metabolites cannot be excluded. In our studies, the reduction of glutamate was observed in glioma cells but not in neural stem cells following Notch blockade (Figure 3C), suggesting the regulation of glutamate metabolism may differ between cancerous and non-cancerous brain stem cells. Finally, our results also suggest utility in monitoring glutamate levels in GBM as a measure of Notch treatment response, as this could potentially be performed non-invasively with ^{1}H-NMR.

Conflict of Interest:

All authors declare no conflict of interest.

Acknowledgment:

UDK is supported by the Dr. Mildred-Scheel post-doctoral fellowship from the

Deutsche Krebshilfe. KK is supported by the Düsseldorf School of Oncology (DSO). The Strategic Research Fund (SFF) and research commission of Heinrich-Heine University Düsseldorf supports the work of JM. This work was funded in part by R01NS055089 to CGE. LM is funded by the grant UL1 TR 001079 from the National Center for Advancing Translational Sciences. UDK wants to thank JP Wu, Baltimore/Charleston for his continuous support.

References:

1. Stupp R, Mason WP, van den Bent MJ, Weller M, Fisher B, Taphoorn MJB, Belanger K, Brandes AA, Marosi C, Bogdahn U, Curschmann J, Janzer RC, et al. Radiotherapy plus concomitant and adjuvant temozolomide for glioblastoma. *N Engl J Med* 2005;352:987–96.

2. Lathia JD, Mack SC, Mulkearns-Hubert EE, Valentim CLL, Rich JN. Cancer stem cells in glioblastoma. *Genes Dev* 2015;29:1203–17.

3. Takebe N, Miele L, Harris PJ, Jeong W, Bando H, Kahn M, Yang SX, Ivy SP. Targeting Notch, Hedgehog, and Wnt pathways in cancer stem cells: clinical update. *Nat Rev Clin Oncol* 2015;

4. Harper JA, Yuan JS, Tan JB, Visan I, Guidos CJ. Notch signaling in development and disease. *Clin Genet* 2003;64:461–72.

5. Aguirre A, Rubio ME, Gallo V. Notch and EGFR pathway interaction regulates neural stem cell number and self-renewal. *Nature* 2010;467:323–7.

6. Allenspach EJ, Maillard I, Aster JC, Pear WS. Notch signaling in cancer. *Cancer Biol Ther* 2002;1:466–76.

7. Teodorczyk M, Schmidt MHH. Notching on Cancer's Door: Notch Signaling in Brain Tumors. *Front Oncol* 2014;4:341.

8. Dang CV. Links between metabolism and cancer. *Genes Dev* 2012;26:877–90.

9. Bi P, Shan T, Liu W, Yue F, Yang X, Liang X-R, Wang J, Li J, Carlesso N, Liu X, Kuang S. Inhibition of Notch signaling promotes browning of white adipose tissue and ameliorates obesity. *Nat Med* 2014;20:911–8.

10. Ciofani M, Zúñiga-Pflücker JC. Notch promotes survival of pre-T cells at the beta-selection checkpoint by regulating cellular metabolism. *Nat Immunol* 2005;6:881–8.

11. Maekawa Y, Ishifune C, Tsukumo S-I, Hozumi K, Yagita H, Yasutomo K. Notch controls the survival of memory CD4+ T cells by regulating glucose uptake. *Nat Med* 2015;21:55–61.

12. Basak NP, Roy A, Banerjee S. Alteration of mitochondrial proteome due to activation of Notch1 signaling pathway. *J Biol Chem* 2014;289:7320–34.

13. Landor SK-J, Mutvei AP, Mamaeva V, Jin S, Busk M, Borra R, Grönroos TJ, Kronqvist P, Lendahl U, Sahlgren CM. Hypo- and hyperactivated Notch signaling induce a glycolytic switch through distinct mechanisms. *Proc Natl Acad Sci U S A* 2011;108:18814–9.

14. Fan X, Khaki L, Zhu TS, Soules ME, Talsma CE, Gul N, Koh C, Zhang J, Li Y-M, Maciaczyk J, Nikkhah G, Dimeco F, et al. NOTCH pathway blockade depletes CD133-positive glioblastoma cells and inhibits growth of tumor neurospheres and xenografts. *Stem Cells Dayt Ohio* 2010;28:5–16.

15. Kahlert UD, Bender NO, Maciaczyk D, Bogiel T, Bar EE, Eberhart CG, Nikkhah G, Maciaczyk J. CD133/CD15 defines distinct cell subpopulations with differential in vitro clonogenic activity and stem cell-related gene expression profile in in vitro propagated glioblastoma multiforme-derived cell line with a PNET-like component. *Folia Neuropathol Assoc Pol Neuropathol Med Res Cent Pol Acad Sci* 2012;50:357–68.

16. Heaphy CM, Schreck KC, Raabe E, Mao XG, An P, Chu Q, Poh W, Jiao Y, Rodriguez FJ, Odia Y, Meeker AK, Eberhart CG. A glioblastoma neurosphere line with alternative lengthening of telomeres. *Acta Neuropathol (Berl)* 2013;126:607–8.

17. Lopez WOC, Nikkhah G, Kahlert UD, Maciaczyk D, Bogiel T, Moellers S, Schültke E, Döbrössy M, Maciaczyk J. Clinical neurotransplantation protocol for Huntington's and Parkinson's disease. *Restor Neurol Neurosci* 2013;31:579–95.

18. Glunde K, Shah T, Winnard PT, Raman V, Takagi T, Vesuna F, Artemov D, Bhujwalla ZM. Hypoxia regulates choline kinase expression through hypoxia-inducible factor-1 alpha signaling in a human prostate cancer model. *Cancer Res* 2008;68:172–80.

19. Schreck KC, Taylor P, Marchionni L, Gopalakrishnan V, Bar EE, Gaiano N, Eberhart CG. The Notch target Hes1 directly modulates Gli1 expression and Hedgehog signaling: a potential mechanism of therapeutic resistance. *Clin Cancer Res Off J Am Assoc Cancer Res* 2010;16:6060–70.

20. Kortenhorst MSQ, Wissing MD, Rodríguez R, Kachhap SK, Jans JJM, Van der Groep P, Verheul HMW, Gupta A, Aiyetan PO, van der Wall E, Carducci MA, Van Diest PJ, et al. Analysis of the genomic response of human prostate cancer cells to histone deacetylase inhibitors. *Epigenetics Off J DNA Methylation Soc* 2013;8:907–20.

21. García-García C, Ibrahim YH, Serra V, Calvo MT, Guzmán M, Grueso J, Aura C, Pérez J, Jessen K, Liu Y, Rommel C, Tabernero J, et al. Dual mTORC1/2 and HER2 blockade results in antitumor activity in preclinical models of breast cancer resistant to anti-HER2 therapy. *Clin Cancer Res Off J Am Assoc Cancer Res* 2012;18:2603–12.

22. Liu J, Pan S, Hsieh MH, Ng N, Sun F, Wang T, Kasibhatla S, Schuller AG, Li AG, Cheng D, Li J, Tompkins C, et al. Targeting Wnt-driven cancer through the inhibition of Porcupine by LGK974. *Proc Natl Acad Sci U S A* 2013;110:20224–9.

23. Wang J-B, Erickson JW, Fuji R, Ramachandran S, Gao P, Dinavahi R, Wilson KF, Ambrosio ALB, Dias SMG, Dang CV, Cerione RA. Targeting Mitochondrial Glutaminase Activity Inhibits Oncogenic Transformation. *Cancer Cell* 2010;18:207–19.

24. Fuerer C, Nusse R. Lentiviral vectors to probe and manipulate the Wnt signaling pathway. *PloS One* 2010;5:e9370.

25. Kahlert UD, Suwala AK, Koch K, Natsumeda M, Orr BA, Hayashi M, Maciaczyk J, Eberhart CG. Pharmacologic Wnt Inhibition Reduces Proliferation, Survival, and Clonogenicity of Glioblastoma Cells. *J Neuropathol Exp Neurol* 2015;74:889–900.

26. Saito N, Fu J, Zheng S, Yao J, Wang S, Liu DD, Yuan Y, Sulman EP, Lang FF, Colman H, Verhaak RG, Yung WKA, et al. A High Notch Pathway Activation Predicts Response to γ Secretase Inhibitors in Proneural Subtype of Glioma Tumor-Initiating Cells. *STEM CELLS* 2014;32:301–12.

27. de Groot J, Sontheimer H. Glutamate and the biology of gliomas. *Glia* 2011;59:1181–9.

28. Zhang K, Zhang J, Han L, Pu P, Kang C. Wnt/beta-catenin signaling in glioma. *J Neuroimmune Pharmacol Off J Soc NeuroImmune Pharmacol* 2012;7:740–9.

29. Bolós V, Grego-Bessa J, de la Pompa JL. Notch signaling in development and cancer. *Endocr Rev* 2007;28:339–63.

30. Gillies RJ, Barry JA, Ross BD. In vitro and in vivo 13C and 31P NMR analyses of phosphocholine metabolism in rat glioma cells. *Magn Reson Med* 1994;32:310–8.

31. Dali-Youcef N, Froelich S, Moussallieh F-M, Chibbaro S, Noël G, Namer IJ, Heikkinen S, Auwerx J. Gene Expression Mapping of Histone Deacetylases and Co-factors, and Correlation with Survival Time and 1H-HRMAS Metabolomic Profile in Human Gliomas. *Sci Rep [Internet]* 2015 [cited 2015 Jul 2];5. Available from: http://www.nature.com/srep/2015/150320/srep09087/full/srep09087.html

32. Righi V, Andronesi OC, Mintzopoulos D, Black PM, Tzika AA. High-resolution magic angle spinning magnetic resonance spectroscopy detects glycine as a biomarker in brain tumors. *Int J Oncol* 2010;36:301–6.

33. Al-Saffar NMS, Marshall LV, Jackson LE, Balarajah G, Eykyn TR, Agliano A, Clarke PA, Jones C, Workman P, Pearson ADJ, Leach MO. Lactate and Choline Metabolites Detected In Vitro by Nuclear Magnetic Resonance Spectroscopy Are Potential Metabolic Biomarkers for PI3K Inhibition in Pediatric Glioblastoma. *PLoS ONE [Internet]* 2014 [cited 2015 Jul 2];9. Available from: http://www.ncbi.nlm.nih.gov/pmc/articles/PMC4118961/

34. Venkatesh HS, Chaumeil MM, Ward CS, Haas-Kogan DA, James CD, Ronen SM. Reduced phosphocholine and hyperpolarized lactate provide magnetic resonance biomarkers of PI3K/Akt/mTOR inhibition in glioblastoma. *Neuro-Oncol* 2012;14:315–25.

35. Kim D, Fiske BP, Birsoy K, Freinkman E, Kami K, Possemato RL, Chudnovsky Y, Pacold ME, Chen WW, Cantor JR, Shelton LM, Gui DY, et al. SHMT2 drives glioma cell survival in ischaemia but imposes a dependence on glycine clearance. *Nature* 2015;520:363–7.

36. Bar EE, Lin A, Mahairaki V, Matsui W, Eberhart CG. Hypoxia increases the expression of stem-cell markers and promotes clonogenicity in glioblastoma neurospheres. *Am J Pathol* 2010;177:1491–502.

37. Jain M, Nilsson R, Sharma S, Madhusudhan N, Kitami T, Souza AL, Kafri R, Kirschner MW, Clish CB, Mootha VK. Metabolite Profiling Identifies a Key Role for Glycine in Rapid Cancer Cell Proliferation. *Science* 2012;336:1040–4.

38. Xu J, Chi F, Guo T, Punj V, Lee WNP, French SW, Tsukamoto H. NOTCH reprograms mitochondrial metabolism for proinflammatory macrophage activation. *J Clin Invest* 2015;125:1579–90.

39. Guidoni L, Ricci-Vitiani L, Rosi A, Palma A, Grande S, Luciani AM, Pelacchi F, di Martino S, Colosimo C, Biffoni M, De Maria R, Pallini R, et al. (1) H NMR detects different metabolic profiles in glioblastoma stem-like cells. *NMR Biomed* 2013;

40. Ramm P, Bettscheider M, Beier D, Kalbitzer HR, Kremer W, Bogdahn U, Hau P, Aigner L, Beier CP. 1H-nuclear magnetic resonance spectroscopy of glioblastoma cancer stem cells. *Stem Cells Dev* 2011;20:2189–95.

41. Angulo-Rojo C, Manning-Cela R, Aguirre A, Ortega A, López-Bayghen E. Involvement of the Notch pathway in terminal astrocytic differentiation: role of PKA. *ASN Neuro* 2013;5:e00130.

42. Chen R, Nishimura MC, Kharbanda S, Peale F, Deng Y, Daemen A, Forrest WF, Kwong M, Hedehus M, Hatzivassiliou G, Friedman LS, Phillips HS. Hominoid-specific enzyme GLUD2 promotes growth of IDH1R132H glioma. *Proc Natl Acad Sci U S A* 2014;111:14217–22.

43. Cuperlovic-Culf M, Ferguson D, Culf A, Morin P, Touaibia M. 1H NMR metabolomics analysis of glioblastoma subtypes: correlation between metabolomics and gene expression characteristics. *J Biol Chem* 2012;287:20164–75.

44. Cassago A, Ferreira APS, Ferreira IM, Fornezari C, Gomes ERM, Greene KS, Pereira HM, Garratt RC, Dias SMG, Ambrosio ALB. Mitochondrial localization and structure-based phosphate activation mechanism of Glutaminase C with implications for cancer metabolism. *Proc Natl Acad Sci* 2012;109:1092–7.

45. Gao P, Tchernyshyov I, Chang T-C, Lee Y-S, Kita K, Ochi T, Zeller KI, De Marzo AM, Van Eyk JE, Mendell JT, Dang CV. c-Myc suppression of miR-23a/b enhances mitochondrial glutaminase expression and glutamine metabolism. *Nature* 2009;458:762–5.

46. Seltzer MJ, Bennett BD, Joshi AD, Gao P, Thomas AG, Ferraris DV, Tsukamoto T, Rojas CJ, Slusher BS, Rabinowitz JD, Dang CV, Riggins GJ. Inhibition of glutaminase preferentially slows growth of glioma cells with mutant IDH1. *Cancer Res* 2010;70:8981–7.

47. Stalnecker CA, Ulrich SM, Li Y, Ramachandran S, McBrayer MK, DeBerardinis RJ, Cerione RA, Erickson JW. Mechanism by which a recently discovered allosteric inhibitor blocks glutamine metabolism in transformed cells. *Proc Natl Acad Sci* 2015;112:394–9.

48. Tanaka K, Sasayama T, Irino Y, Takata K, Nagashima H, Satoh N, Kyotani K, Mizowaki T, Imahori T, Ejima Y, Masui K, Gini B, et al. Compensatory glutamine metabolism promotes glioblastoma resistance to mTOR inhibitor treatment. *J Clin Invest* 2015;125:1591–602.

Figure Legends:

Figure 1: Glioma cell lines with different sensitivity to Notch blockade with MRK003: Confirmation of successful suppression of Notch signaling through inhibition of transcription of canonical pathway targets *HES1* and *HEY1* distinguishes between MRK003 sensitive (GBM1, GBM10 and GBM14) and insensitive (U87NS and 040922) cells (A, p-value≤0.05). This treatment led to minimal induction of apoptosis in GBM1 (21% to 27% AnnexinV positive cells) and had no effect on GBM10, U87NS and 040922 (B, p-value≤0.05).

Figure 2: Global metabolic profiling of GBM neurospheres after MRK003 administration with proton magnetic resonance spectroscopy (^{1}H-NMR): Assessing the metabolic composition of *in vitro* metabolic extracts of glioma cells sensitive (GBM1) and insensitive (U87NS) to MRK003 via ^{1}H-NMR with and without drug exposure identified various metabolites including valine/ isoleucine (Val/Iso), threonine (Thr), lactate (Lac), alanine (Ala), N-Acetylaspartylglutamat (NAAG), glutamate (Glu), glutamine (Gln), glutathione (GSH), total creatine (tCre), free choline (fCho), phosphocholine (PC), glycerophosphocholine (GPC), glycine (Gly) and *myo*-inositol (myo) (A). Quantification of three independent rounds for each represented as mean plus SEM (B) (p-value≤0.05).

Figure 3: Reduction of intracellular glutamate after Notch blockade: MRK003 sensitive GBM1 reduces levels of intracellular glutamate but not in MRK003 insensitive U87NS cells as assessed with ^{1}H-NMR (A). In addition, MRK003 sensitive cells GBM1 and GBM10 exhibit lower intracellular glutamate levels after Notch blockade as confirmed with glutamate dehydrogenase-mediated quantification of glutamate oxidation which was not seen in MRK003 insensitive U87NS and 040922 (B). Notch blockade did not reduce glutamate in human fetal neural stem cells as assessed with the ELISA kit (C) (p-value≤0.05).

Figure 4: Other chemotherapeutic treatments did not reduce levels of glutamate: Administration of alkylating agent Temozolomid (TMZ) or mTOR inhibitor MLN0128 (MLN) significantly impaired glioma cell growth as shown for MRK003 sensitive cell lines GBM1 and

GBM10 (A). Treatment with TMZ and MLN for 48 hours induced apoptosis for GBM1 but not for GBM10 while glutamate levels remained unchanged (B). Porcupine inhibitor LGK974 inhibited transcriptional activity of WNT/beta-catenin signaling in GBM1 and LN229 but had no significant effect on glutamate (C) (p-value≤0.05).

Figure 5: MRK003 modulates expression of multiple genes regulating glutamate homeostasis: Micro-array analysis of MRK003 sensitive cells GBM1, GBM10 and GBM14 after suppression of Notch revealed the altered expression of multiple genes involved in glutamate homeostasis (A). RT PCR based quantification of mRNA transcription confirmed the suppression of genes involved in glutamate metabolism after Notch blockade including glutamate carboxypeptidase II (*GCPII*), soluble carrier (SLC) membrane transporter *SLC1A3* as well as kidney type glutaminase (*GLS1*) in MRK003 sensitive glioma neurospheres but not in MRK003 insensitive cultures. (B). MRK003 sensitive cells have higher baseline expression of glutaminase as compared to MRK003 insensitive cells (C) (p-value≤0.05).

Figure 6: Treatment with pharmacological inhibitor of glutaminase compound 968 can slow glioma cell growth in MRK003 sensitive but not in MRK003 insensitive cells (A, p-value≤0.05). No additive effect of MRK003 in combination with compound 968 on cell growth was observed (Figure B, day 4 for fast growing GBM1, day 6 for GBM10, p-value≤0.05).

Supporting Data File S1: Short tandem repeat profiles of cell lines used in this study.

Supporting Data File S2: Primer sequences used for RT qPCR in this study.

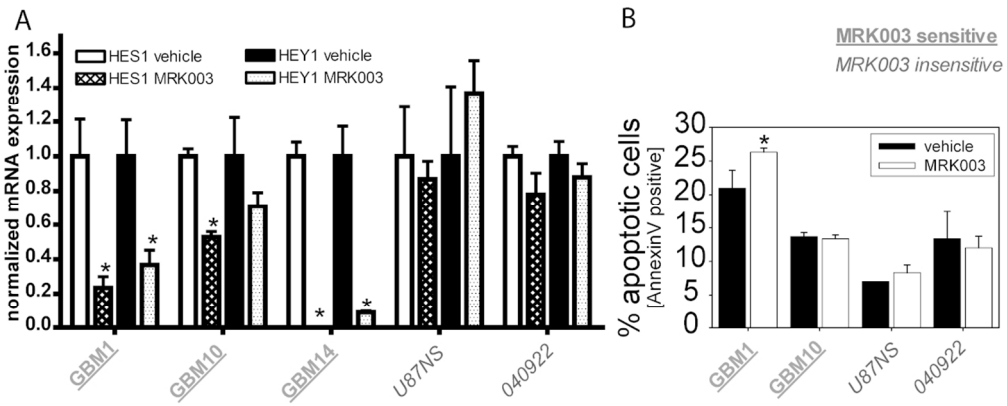

Figure 1: Glioma cell lines with different sensitivity to Notch blockade with MRK003: Confirmation of successful suppression of Notch signaling through inhibition of transcription of canonical pathway targets HES1 and HEY1 distinguishes between MRK003 sensitive (GBM1, GBM10 and GBM14) and insensitive (U87NS and 040922) cells (A, p-value≤0.05). This treatment led to minimal induction of apoptosis in GBM1 (21% to 27% AnnexinV positive cells) and had no effect on GBM10, U87NS and 040922 (B, p-value≤0.05).
216x87mm (150 x 150 DPI)

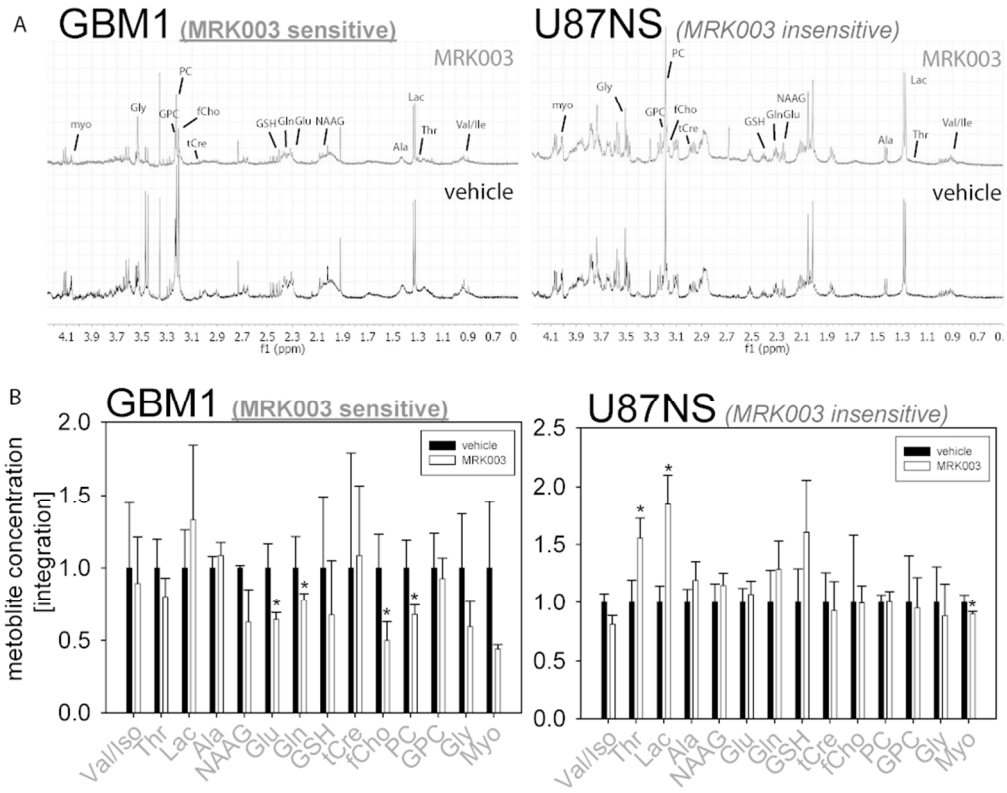

Figure 2: Global metabolic profiling of GBM neurospheres after MRK003 administration with proton magnetic resonance spectroscopy (1H-NMR): Assessing the metabolic composition of in vitro metabolic extracts of glioma cells sensitive (GBM1) and insensitive (U87NS) to MRK003 via 1H-NMR with and without drug exposure identified various metabolites including valine/ isoleucine (Val/Iso), threonine (Thr), lactate (Lac), alanine (Ala), N-Acetylaspartylglutamat (NAAG), glutamate (Glu), glutamine (Gln), glutathione (GSH), total creatine (tCre), free choline (fCho), phosphocholine (PC), glycerophosphocholine (GPC), glycine (Gly) and myo-inositol (myo) (A). Quantification of three independent rounds for each represented as mean plus SEM (B) (p-value≤0.05).
174x138mm (150 x 150 DPI)

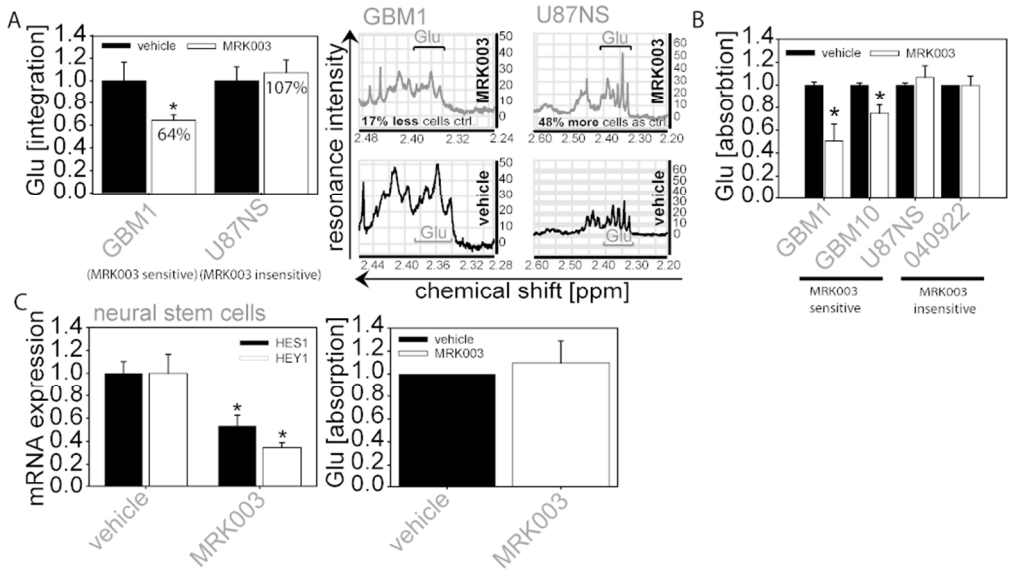

Figure 3: Reduction of intracellular glutamate after Notch blockade: MRK003 sensitive GBM1 reduces levels of intracellular glutamate but not in MRK003 insensitive U87NS cells as assessed with 1H-NMR (A). In addition, MRK003 sensitive cells GBM1 and GBM10 exhibit lower intracellular glutamate levels after Notch blockade as confirmed with glutamate dehydrogenase-mediated quantification of glutamate oxidation which was not seen in MRK003 insensitive U87NS and 040922 (B). Notch blockade did not reduce glutamate in human fetal neural stem cells as assessed with the ELISA kit (C) (p-value≤0.05).
174x99mm (150 x 150 DPI)

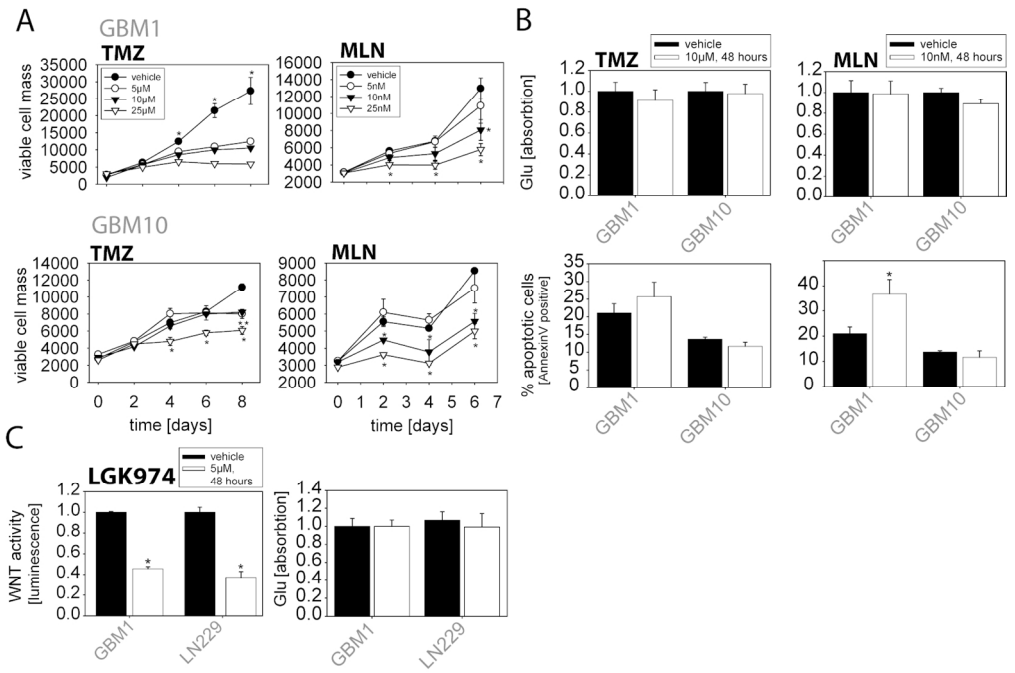

Figure 4: Other chemotherapeutic treatments did not reduce levels of glutamate: Administration of alkylating agent Temozolomid (TMZ) or mTOR inhibitor MLN0128 (MLN) significantly impaired glioma cell growth as shown for MRK003 sensitive cell lines GBM1 and GBM10 (A). Treatment with TMZ and MLN for 48 hours induced apoptosis for GBM1 but not for GBM10 while glutamate levels remained unchanged (B). Porcupine inhibitor LGK974 inhibited transcriptional activity of WNT/beta-catenin signaling in GBM1 and LN229 but had no significant effect on glutamate (C) (p-value≤0.05).
278x187mm (150 x 150 DPI)

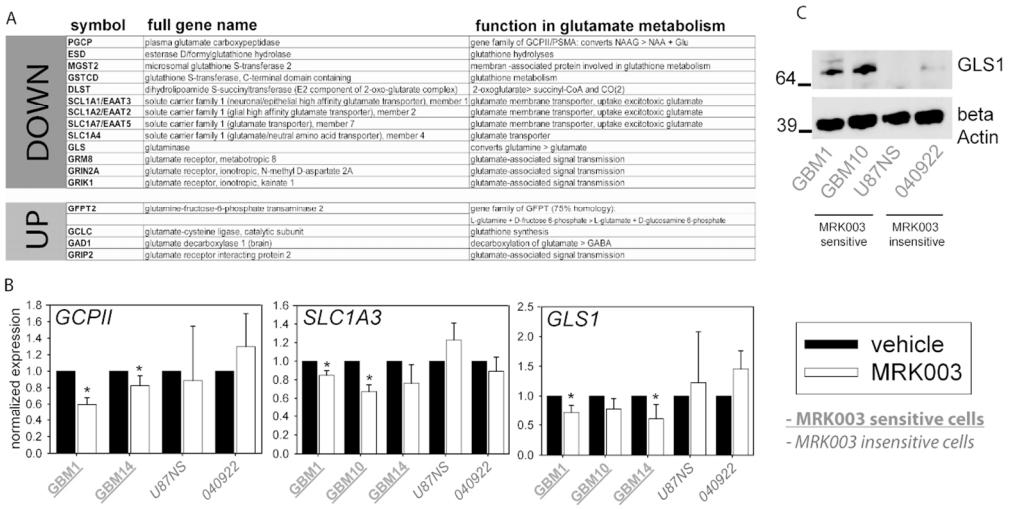

Figure 5: MRK003 modulates expression of multiple genes regulating glutamate homeostasis: Micro-array analysis of MRK003 sensitive cells GBM1, GBM10 and GBM14 after suppression of Notch revealed the altered expression of multiple genes involved in glutamate homeostasis (A). RT PCR based quantification of mRNA transcription confirmed the suppression of genes involved in glutamate metabolism after Notch blockade including glutamate carboxypeptidase II (GCPII), soluble carrier (SLC) membrane transporter SLC1A3 as well as kidney type glutaminase (GLS1) in MRK003 sensitive glioma neurospheres but not in MRK003 insensitive cultures. (B). MRK003 sensitive cells have higher baseline expression of glutaminase as compared to MRK003 insensitive cells (C) (p-value≤0.05).
225x114mm (150 x 150 DPI)

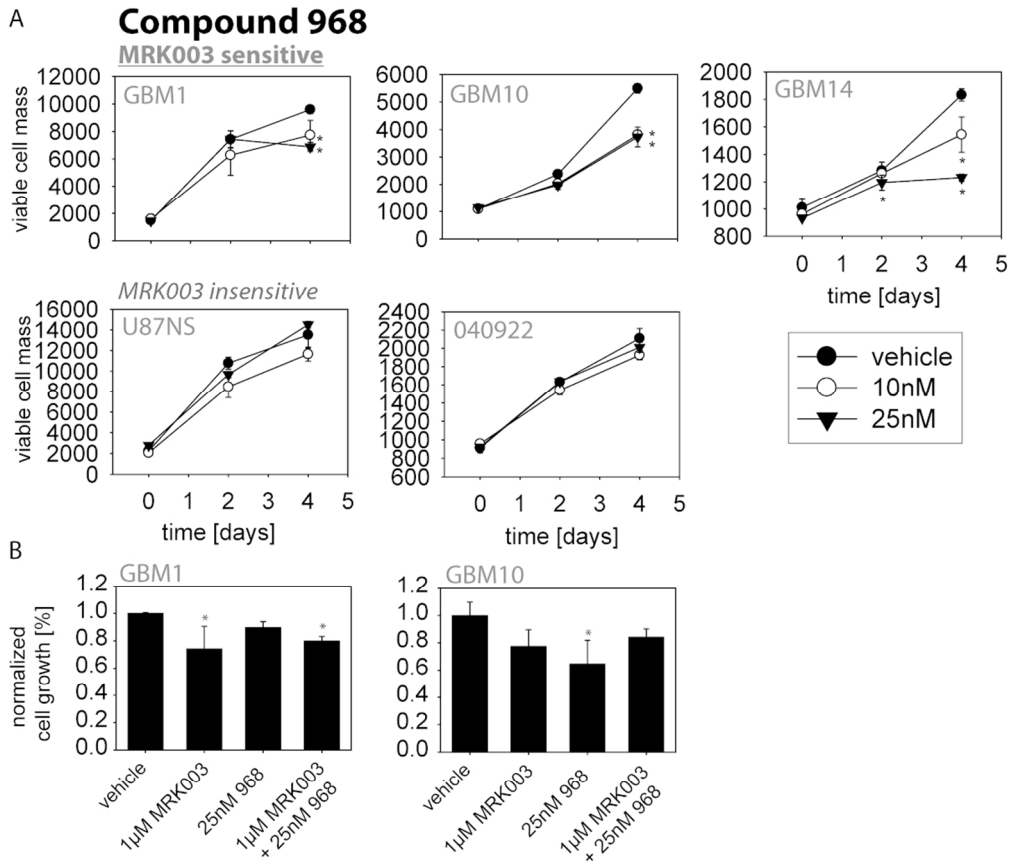

Figure 6: Treatment with pharmacological inhibitor of glutaminase compound 968 can slow glioma cell growth in MRK003 sensitive but not in MRK003 insensitive cells (A, p-value≤0.05). No additive effect of MRK003 in combination with compound 968 on cell growth was observed (Figure B, day 4 for fast growing GBM1, day 6 for GBM10, p-value≤0.05).
202x177mm (150 x 150 DPI)